Journal of Applied Mechanics and Technical Physics, Vol. 48, No. 6, pp. 840–851, 2007

FINE STRUCTURE OF A STRATIFIED FLOW NEAR A FLAT-PLATE SURFACE

R. N. Bardakov, V. V. Mitkin, and Yu. D. Chashechkin

UDC 551.466.6:523.527

The pattern of disturbances arising during the motion of a strip along a horizontal surface in a continuously stratified fluid with identified upstream and attached internal waves, boundary layers, and edge singularities is calculated in the liner approximation. The flow pattern behind a flat plate moving with a constant velocity in a continuously stratified fluid is studied with the use of the optical schlieren technique; transformation of waves and finely structured elements of the flow with increasing plate velocity is analyzed. The calculated and experimentally observed patterns of internal waves at low velocities are demonstrated to be in good agreement.

Key words: *stratified fluid, waves, wake, streaky structures.*

The interest in studying the fluid flow structure near streamlined obstacles, which was discussed in numerous theoretical and experimental papers (see, e.g., [1, 2]), has been recently revived owing to the search for mechanisms of formation of streaky structures in the boundary layer [3] and vortex loops in the flow [4]. Particular attention is paid to studying the flow past a flat plate aligned in the mean flow direction. Initial inhomogeneities are generated by inserting mechanical, acoustic, or thermal perturbations into the uniform flow in the wind tunnel. The streaks and vortex structures arising in the boundary layer on a flat plate are visualized by numerical methods with the use of hot-wire measurements of the flow and essential assumptions on the flow character [4, 5].

In addition to contact methods, the optical schlieren technique is also used to study gas flows and flows of an inhomogeneous fluid, because even comparatively small variations of density $\Delta\rho$ ($\Delta\rho/\rho_0 \ll 10^{-4}$–$10^{-7}$) lead to significant changes in the refractive index n ($\Delta n/n \sim 10^{-5}$–10^{-8}) [6].

Transverse streaky structures whose thin elements are aligned at an angle to the flow direction were visualized by means of the schlieren technique in a continuously stratified fluid in an immediate vicinity of a horizontal plate [7] with flow velocity much smaller than that used in [4]. As the velocity is increased, uniformly distributed transverse streaks are grouped into clusters, the latter being transformed to a vortex street with distance from the obstacle [8]. Streaky structures were also observed in the boundary layer on the side surface of a vertically moving cylinder [9]. In repeated experiments [7–9], with no additional disturbances introduced into the flow, all large-scale and small-scale elements of the flow are well reproduced. The experimental results [4, 7–9] demonstrate that a more detailed mathematical analysis of comparatively slow stratified flows past a flat plate is needed. At the first stage, it is reasonable to use linear models, which effectively describe internal waves with allowance for dissipative factors: fluid viscosity and diffusion of the stratifying component [6].

In the general case, linearized three-dimensional equations of fluid motion describe two types of flow elements singular in terms of viscosity, whose thickness depends on the problem geometry [10]. As the equations are nonlinear, the structural elements of the flow interact with each other and can generate new waves and vortex systems.

The objective of the present work is to compare experimental and calculated (in the linear formulation) patterns of a stratified flow on a flat plate and to visualize the flow in a wide range of parameters, including laminar and transitional regimes.

Institute for Problems in Mechanics, Russian Academy of Sciences, Moscow 119526; chakin@ipmnet.ru.
Translated from Prikladnaya Mekhanika i Tekhnicheskaya Fizika, Vol. 48, No. 6, pp. 77–91, November–December, 2007. Original article submitted July 11, 2006; revision submitted November 9, 2006.

Governing Equations, Characteristic Scales, and Dimensionless Parameters of the Problem. The density of a weakly compressed fluid stratified in terms of salinity $S(z)$, which changes in an undisturbed state only in the vertical direction z according to the law

$$\rho(z,t) = \rho(S(z,t)) \approx \rho_0[1 + \beta S(z,t)] \tag{1}$$

is characterized by the scale $\Lambda = |(1/\rho_0)\, d\rho_0/dz|^{-1}$, frequency $N = \sqrt{g/\Lambda}$, and buoyancy period $T_b = 2\pi/N$. In what follows, the salinity definition is supplemented by a salt compression coefficient β, while the buoyancy scale is assumed to be constant.

The system of equations of motion includes the equations of state (1), Navier–Stokes equations, and equations of incompressibility and conservation of the stratified component (salinity S):

$$\begin{gathered}
\rho\Big(\frac{\partial \boldsymbol{v}}{\partial t} + (\boldsymbol{v}\,\nabla)\boldsymbol{v}\Big) = -\nabla P + \rho\nu\,\Delta\boldsymbol{v} + \rho\boldsymbol{g}, \\
\frac{\partial \rho}{\partial t} + \boldsymbol{v}\,\nabla\rho = 0, \\
\frac{\partial S}{\partial t} + (\boldsymbol{v}\,\nabla)S = \varkappa_S\,\Delta S, \qquad S = S_0(z) + S'(x,y,z,t), \\
div\boldsymbol{v} = 0, \qquad \rho(z) = \rho(S(z)).
\end{gathered} \tag{2}$$

Here $\boldsymbol{v}$ is the velocity, P is the pressure, t is the time, $\boldsymbol{g}$ is the acceleration of gravity, and ν, $\varkappa_S$, and β are the kinematic viscosity, salt diffusion coefficient, and salt compression coefficient, respectively, which are assumed to be constant.

The source of disturbances in the fluid is a strip of length L_x moving with a velocity U along the normal to its edge along an infinite quiescent horizontal plane. The boundary conditions are the no-slip conditions for velocity, no-flux conditions for the substance, and decay of disturbances at infinity.

The problem has several length scales; the greatest of them are the buoyancy scale Λ, strip length L_x, and the length of the attached internal wave $\lambda = UT_b = 2\pi U/N$. The viscous wave scale $L_\nu = \sqrt[3]{g\nu}/N$ characterizes the relative size of the flat plate L_x/L_ν responsible for the interference structure of the wave field. The universal microscales $\delta_N = \sqrt{\nu/N}$ and $\delta_S = \sqrt{\varkappa_S/N}$, which characterize the boundary-layer thickness in an unsteady flow induced by diffusion on a non-permeable obstacle [11] and the thickness of periodic boundary layers on the oscillating surface [12], may be manifested in structures of the flow fields near the uniformly moving plate. Shear boundary layers are formed on contact surfaces, which are characterized by the length scales $\delta_u = \nu/U$ and $\delta_\rho = \varkappa_S/U$ typical of the Prandtl and Peclet models [2].

The ratios of the basic scales form the main dimensionless parameters of stratified flows, which reflect the relative influence of dissipative factors (Reynolds number $\mathrm{Re} = L_x/\delta_u = UL_x/\nu$, Peclet number $\mathrm{Pe} = L_x/\delta_\rho = UL_x/\varkappa_S$, or Schmidt number $\mathrm{Sc} = \mathrm{Pe}\,/\,\mathrm{Re} = \nu/\varkappa_S$), buoyancy effects (internal Froude number $\mathrm{Fr} = \lambda/(2\pi L_x) = U/(NL_x)$), and changes in density on the scales of the obstacles (the ratio of the scales $C = \rho_0/\Delta\rho = \Lambda/L_x$).

In the linear model [8, 11, 12], the singular elements not only identify the region near the obstacle with a significant effect of dissipative factors but take an active part in flow reconstruction in the depth of the fluid. Like waves, the singular components (boundary layers) exist for all finite velocities of the flow. Even if there are no external disturbing factors, stratified media contain flows induced by diffusion on a motionless obstacle [11]. The fact of merging and degeneration of three-dimensional boundary layers of different nature [10, 13], which makes the analysis of equations in the approximation of a homogeneous fluid more difficult, has not been analyzed previously.

As stratification is usually rather weak ($\Delta\rho/\rho \ll 1$ and $C \gg 1$), and the kinetic coefficients are rather small, the values of the basic scales are essentially different ($\Lambda \gg D \gg \delta_u \gg \delta_\rho$ and $\lambda \gg \delta_N \gg \delta_S$). The smallest basic scale among the set of basic scales (δ_ρ or δ_S) defines the spatial resolution of the method necessary for registration of flow elements over the entire flow field.

Calculation of Flow Parameters near the Plate in the Linear Approximation. To construct the exact solution of the two-dimensional problem, we linearize system (2) and reduce it to a standard equation of internal waves in a viscous medium for the stream function Ψ and perturbations of salinity S. The solution is sought in the form of expansions into the Fourier integrals over plane waves of the form $A = A_0 \exp[i(\boldsymbol{kr} - \omega t)]$,

where $\boldsymbol{k} = (k_x, k_y, k_z)$ is the wave vector whose components contain real and imaginary parts, A is the component of velocity of the pressure (density) perturbation, A_0 is the component of the disturbance amplitude, ω is the frequency (which is real and positive), and $\boldsymbol{r}$ is the radius vector.

From the condition of existence of a nontrivial solution of the linearized version of system (2), there follows a dispersion equation whose solutions are divided into two types: regular solutions and singular solutions in terms of viscosity [10].

In a viscous fluid, the system of internal waves described by regular roots of the solution of the dispersion equation is supplemented by two types of the boundary layers, which correspond to singular solutions. The properties of a diffusion boundary layer are determined by the diffusion coefficient [12]. Two other boundary layers (Stokes isopycnic and internal ones) exist in a viscous medium, the effects of diffusion being neglected [10, 13, 14].

In the problem of generation of waves by a strip moving in the horizontal plane, the dispersion equation [12] in the Boussinesq approximation acquires the form

$$(\omega + i\nu\boldsymbol{k}^2)(\omega + i\varkappa_S\boldsymbol{k}^2)(N^2k_x^2 - \omega\boldsymbol{k}^2(\omega + i\nu\boldsymbol{k}^2)) = 0,$$

where the first two terms characterize the diffusion and isopycnic (Stokes) boundary layers, and the third term describes the field of internal waves and the internal boundary layer. The multiplicative form of the dispersion equation means that the boundary layers are completely split in this case. As we have $\mathrm{Sc} \gg 1$ in the aqueous solution of cooking salt, we can neglect the influence of diffusion effects on the flow pattern at the first stage of calculations and analyze the velocity field in a two-dimensional statement.

Under the assumptions made, system (2) reduces to the equation for the stream function Ψ whose derivatives define the fluid velocity components $v_x = \partial\Psi/\partial z$ and $v_z = -\partial\Psi/\partial x$ [1]:

$$\Big[\frac{\partial^2}{\partial t^2}\Big(\frac{\partial^2}{\partial x^2} + \frac{\partial^2}{\partial z^2}\Big) + N^2\,\frac{\partial^2}{\partial x^2} - \nu\,\frac{\partial}{\partial t}\Big(\frac{\partial^2}{\partial x^2} + \frac{\partial^2}{\partial z^2}\Big)^2\Big]\Psi = 0 \tag{3}$$

with the no-slip boundary conditions on the solid surface and decay of all disturbances at infinity. The standard no-slip boundary conditions on the entire infinite horizontal plane along which a strip of length L_x moves perpendicular to its own leading edge with a velocity U acquire the form

$$\frac{\partial\Psi}{\partial z}\Big|_{z=0} = U\theta\Big(x + \frac{L_x}{2} - Ut\Big)\theta\Big(\frac{L_x}{2} + Ut - x\Big), \qquad \frac{\partial\Psi}{\partial x}\Big|_{z=0} = 0, \tag{4}$$

where θ is the Heaviside function.

We seek for the solution of Eq. (3) by the method of expansion into the Fourier series:

$$\Psi(x,z,t) = \int\limits_{-\infty}^{\infty} \mathrm{e}^{-i\omega t} \int\limits_{-\infty}^{\infty} \Big(A_w\,\mathrm{e}^{ik_{z,w}z} + B_i\,\mathrm{e}^{ik_{z,i}z}\Big)\,\mathrm{e}^{ik_x x}\;dk_x\,d\omega. \tag{5}$$

In calculating Eq. (5), we take into account the roots of the dispersion equation, which satisfy the condition of decay of disturbances at infinity. Equation (3) corresponds to the fourth-order algebraic dispersion equation

$$\omega^2\boldsymbol{k}^2 - N^2k_x^2 + i\omega\nu\boldsymbol{k}^4 = 0, \tag{6}$$

whose roots ($k_{z,w}$ and $k_{z,i}$) are chosen from the conditions of decay of disturbances at infinity. The roots are chosen so that the spectral coefficient $A_w(\omega, k_z)$ describes the field of internal waves and the coefficient $B_i(\omega, k_z)$ describes the internal boundary layer.

The root of Eq. (6) regular in terms of viscosity

$$k_{z,w}^2(\omega, k_x) = -k_x^2 + i\omega\Big(1 - \sqrt{1 + 4i\nu k_x^2N^2/\omega^3}\Big)/(2\nu) \tag{7}$$

(the main term of the expansion $\mathrm{Im}\,k_w \sim \nu^\alpha$, $\alpha > 0$) characterizes internal waves. As $\nu \to 0$, solution (7) transforms to the known solution of the dispersion equation for an ideal fluid [6].

The root

$$k_{z,i}^2(\omega, k_x) = -k_x^2 + i\omega\Big(1 + \sqrt{1 + 4i\nu k_x^2N^2/\omega^3}\Big)/(2\nu) \tag{8}$$

is singular in terms of viscosity (in the main term of the expansion $\mathrm{Im}\,k_b \sim \nu^{-1/2}$) and characterizes the internal boundary layer. With allowance for Eqs. (7) and (8), solution (5) allows one to calculate all characteristics of the flow.

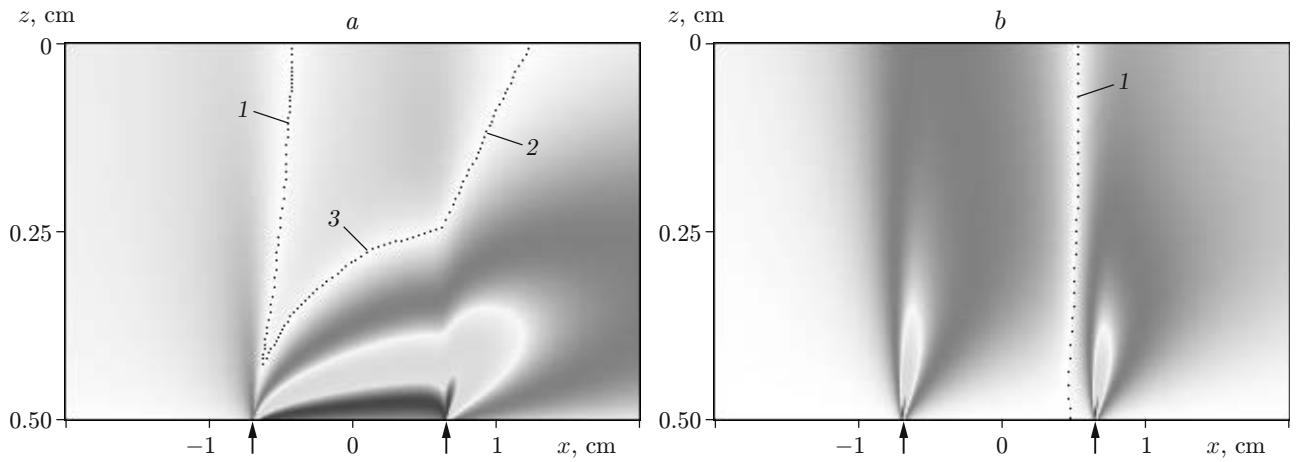

Fig. 1. Absolute values of the horizontal (a) and vertical (b) velocity components near a short plate ($T_b = 14$ sec, $L_x = 2$ cm, $U = 1$ cm/sec, $\lambda = 14$ cm, Fr = 1.12, Re = 200, and $C = \Lambda/L_x = 2435$): curves 1–3 show the zero values of velocity at the crests of internal waves (1), troughs of internal waves (2), and outer edge of the boundary layer (3); the arrows indicate the positions of the leading and trailing edges of the flat plate.

The spatial structure of the field of internal waves excited by the uniformly moving plate was analyzed in [14] for different relations between the wave length, plate size, and boundary-layer thickness. Numerical visualization of the flow in the vicinity of the plate is also of interest.

To construct the flow pattern, we used the Simpson method to calculate the values of integrals (5) and the components of the velocity vector at grid nodes; the grid step was chosen from the condition of resolving of the velocity boundary layer (up to 10 points at the scale $\delta_\nu = \nu/U$). With the help of a code written by the present authors in the MS Visual C++ environment, the data obtained were used to construct the colored image of various physical fields. The present paper contains the transformed black-and-white versions of the images, which hinders identification of some details that are clearly visible in the original colored images.

The calculated flow pattern in the vicinity of a short plate whose length is smaller than the viscous wave scale $L_\nu = \sqrt[3]{g\nu}/N = 2.7$ cm and the wave length $\lambda = UT_b = 14$ cm is shown in Fig. 1 in the laboratory coordinate system fitted to the motionless fluid (the plate in Figs. 1–7 moves from right to left).

The structure of the field of the absolute values of the horizontal velocity component contains several typical elements: singularities in the vicinity of the leading and trailing edges, boundary layer of the Prandtl type, and phase surfaces of internal waves (curves 1–3 in Fig. 1 show the geometric locations of the points with the zero velocity of the fluid). A comparison with results of previous calculations of the flow past a strip shows that curves 1 and 2 characterize the positions of the crests and troughs of internal waves for this component of flow velocity.

The curve of zero velocities 3 refers to the outer edge of the boundary layer formed by the sum of regular and singular components of the flow above the plate. In contrast to a uniform fluid, where the boundary-layer thickness δ_ν depends on the method of its determination (criteria of one-percent and half-percent velocity deficit at the boundary are used in practice: $1 - u(\delta_\nu)/U = 0.005$ [15]), the curve of the zero values of velocity along the plate in a stratified fluid rigorously determines the position of the outer edge of the boundary layer. The change in the sign of velocity disturbances is caused by the existence of internal waves in the entire space of the periodic field. The boundary-layer thickness monotonically increases along the plate. The singularity of the trailing edge is more pronounced than the singularity of the leading edge.

The edge singularities are also more clearly expressed in the field of the vertical velocity component (Fig. 1b). The fluid is pushed away from the plate near the leading edge and returns to the initial level near the trailing edge. The position of the curves of the zero value of the vertical velocity component near the plate (curve 1 in Fig. 1b) is determined by the phase structure of the field of internal waves.

A comparison of Figs. 1a and 1b shows that the flow patters near the plate in different variables are as different as in the field of internal waves far from the plate. A comparison of the flow patterns in Fig. 1 and in [14] shows that effective sources of waves are edge singularities responsible for the shift of density isolines and emergence

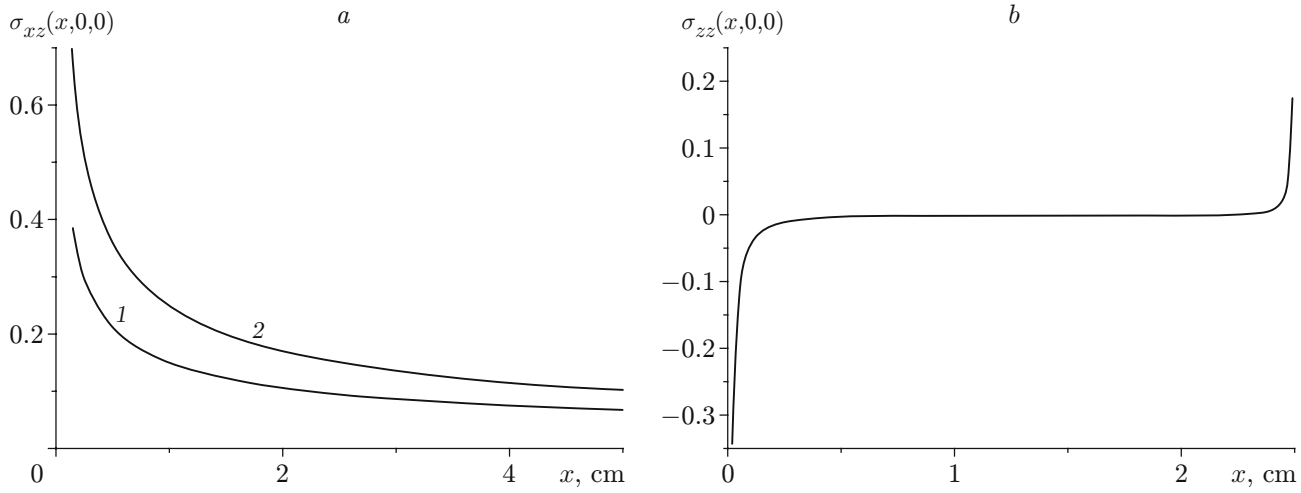

Fig. 2. Distributions of the viscous stress tensor components along the strip ($U = 0.17$ cm/sec and $T_b = 7.55$ sec): (a) $L_x = 400$ cm; curves 1 and 2 refer to the calculations performed by formula (9) in the approximation of a homogeneous and stratified fluids, respectively; (b) $L_x = 2.5$ cm.

of unsteady upstream and steady downstream (leeward) internal waves. Thus, the spatial inhomogeneity of the field of wave disturbances is explained by superposition of two types of waves from different sources.

Two groups of unsteady waves generated by the leading and trailing edges of the plate are formed ahead of the plate. The interference wave pattern above the side surface of the plate is the result of summation of steady attached waves generated by the leading edge and unsteady waves generated by the trailing edge (see also [14]). The two systems of steady attached waves overlap in the region behind the plate. The degree of manifestation of edge singularities depends on flow parameters. Normally, the leading edge is a more effective source of waves than the trailing edge.

The structure of the velocity field near the plate reflects the influence of the friction force acting in the mean flow direction and the moment of forces with respect to the plate center. The component σ_{xz} of the viscous stress tensor determines the drag force normalized to the unit area of the surface:

$$\sigma_{xz}(x,z,t) = -\frac{i\nu U}{\pi}\int\limits_{-\infty}^{\infty}\frac{1}{k_x}\sin\frac{k_x a}{2}\,\mathrm{e}^{ik_x(x-Ut)}\,\frac{k_{z,w}^2\,\mathrm{e}^{ik_{z,w}z}-k_{z,i}^2\,\mathrm{e}^{ik_{z,i}z}}{k_{z,w}-k_{z,i}}\,dk_x. \tag{9}$$

The edge singularities generate a pair of forces characterized by the component σ_{zz} of the viscous stress tensor:

$$\sigma_{zz}(x,z,t) = \frac{i\nu U}{\pi}\int\limits_{-\infty}^{\infty}\sin\frac{k_x a}{2}\,\mathrm{e}^{ik_x(x-Ut)}\,\frac{k_{z,w}\,\mathrm{e}^{ik_{z,w}z}-k_i\,\mathrm{e}^{ik_{z,i}z}}{k_{z,w}-k_{z,i}}\,dk_x.$$

The calculated values of σ_{xz} and σ_{zz} for the long and short plates are plotted in Fig. 2. The values of the running friction force calculated by formula (9) in the approximations of homogeneous fluid (curve 1 in Fig. 2a) and stratified fluid (curve 2) differ near the edges, almost coincide in the central part of the long plate, where the influence of edge singularities is insignificant, and agree with the calculations by the Prandtl–Blasius model, despite significant differences in problem formulations ($F_x = 0.332\sqrt{\eta\rho U^3/x}$ [2]).

Figure 2b shows the component σ_{zz} calculated for the short plate. It is seen that the moment induced solely by the action of edge singularities is responsible for descending of the leading edge and ascending of the trailing edge. Similar forces affect each side of the plate moving in free space. The absence of the moment of forces at a zero angle of attack of the free plate in the flow is a consequence of exact compensation of moments acting on each side of the plate in the Boussinesq approximation. The balance is violated by allowance for changes in density in exact equations or by deviation of the plate position from the horizontal one.

The nonlinear terms in the full system (2) characterize the interaction of both regular and singular elements of the flow. The interaction of singular elements is primarily manifested near the plate, leading to formation of vortex elements and complicating the flow structure. As the velocity shear reaches the maximum values near the plate, the results of interaction of singular components start to manifest themselves already at comparatively low velocities and lead to formation of new structural (vortex) elements.

To register the elements of the flow field with the scales $\delta_u = \nu/U$ and $\delta_N = \sqrt{\nu/N}$, one has to use field methods with high sensitivity and resolution. Commercial optical schlieren instruments satisfy these requirements.

Experimental Technique. The experiments were performed in a tank $220 \times 40 \times 60$ cm with optical illuminators built into the side walls. By the method of continuous displacement, the tank was filled by a stratified solution of cooking salt. The homogeneity and the buoyancy period were monitored by observations of fluid oscillations excited by a density marker (submerging salt or sugar crystal); the measurements were performed by a contact electrical conductivity gauge, with the marker being formed in the vicinity of the gauge sensor. The error of the direct measurement of the buoyancy period was less than 5% [16].

Above the tank, there was a carriage, which was towed along the guides with a velocity $U = 0.08$–5.00 cm/sec. A horizontal rectangular plate was attached to the carriage with the help of vertical knives whose lower part was made of thin transparent plastic. The horizontal position of the plate and its trajectory with respect to the water surface in the period of tank filling were carefully monitored. The plates used for experiments were 0.1 cm thick, 36.5 cm wide, and had a length $L_x = 2.5$ or 7.5 cm. The range of experimental parameters corresponds to the laminar and transitional (vortex) flow regimes.

The observations were performed by an IAB-458 schlieren instrument with a white light source. For refraction effects caused by light dispersion in the working medium to be reduced, the illumination slot was aligned vertically. The diaphragms forming the schlieren pictures were the Foucault knife or a filament, which were also mounted vertically. The method of the Foucault knife is characterized by high sensitivity, while the method with the filament is more informative, because it allows one to distinguish the wave crests and troughs and to visualize thin high-gradient interfaces on the background of intense internal waves.

Basic Results. Superposition of images visualized by the method with the filament and the calculated flow patterns formed during the motion of the horizontal flat plate with small and moderate velocities shows that the structures of the phase surfaces of internal waves are in good agreement (Fig. 3). The experimentally observed pattern shows both the upstream unsteady waves (inclined beams ahead of the body) and the steady attached internal waves (deformed semicircles behind the plate whose edges are marked by the arrows). In the lower part of Fig. 3a, the deformed vertical lines show the density markers formed by freely submerging crystals of sugar, which were used to visualize the horizontal component of fluid velocity. The points where the markers change the direction of their motion coincide with wave crests and troughs. For low Froude numbers, the most intense disturbance arises ahead of the obstacle, while the disturbance behind the obstacle is weaker.

Directly above the plate, where unsteady and steady waves from different sources overlap, the wave field has a complicated structure, and the non-local character of the source is manifested even in the flow field above the short plate. Distortions of the shape of wave surfaces above the plate become less intense with distance (Fig. 3a). With increasing velocity, the wave length increases, the contact point between the first wave crest and the plate is shifted toward the trailing edge (Fig. 3b), and a system of short thin disturbances aligned at an angle to the velocity direction is formed near the plate. The system of these disturbances is called the transverse streaky structure. Some streaks are directed along the streamlines near the plate and along its hydrodynamic wake. The schlieren picture above the long plate shows a deflection of the phase surfaces (see lower part of Fig. 4a) and their discontinuity in the calculated field of the signature (sign) of the vertical velocity component (in light regions, the velocity is directed away from the plate). The positions of the lines of phase changes and the points of their contact with the plane of motion depends on flow parameters. At low velocities ($L_x/\lambda = 10$), the main disturbance is located ahead of the source [6], and the wave pattern has only one clearly expressed line of the phase change, which is aligned at an angle of 120° to the line of motion and contacts the plate at a distance of approximately 1.2 cm from the leading edge (Fig. 4a). For greater velocities and wave lengths ($L_x/\lambda = 3$), the interference pattern displays two lines of the phase change located at an angle of 60° to the line of motion (Fig. 4b).

In the region behind the plate, with only steady attached waves, the phase surfaces deviate from the calculated semicircles in an immediate vicinity of the plane of motion of the source. The deformation of the wave crests

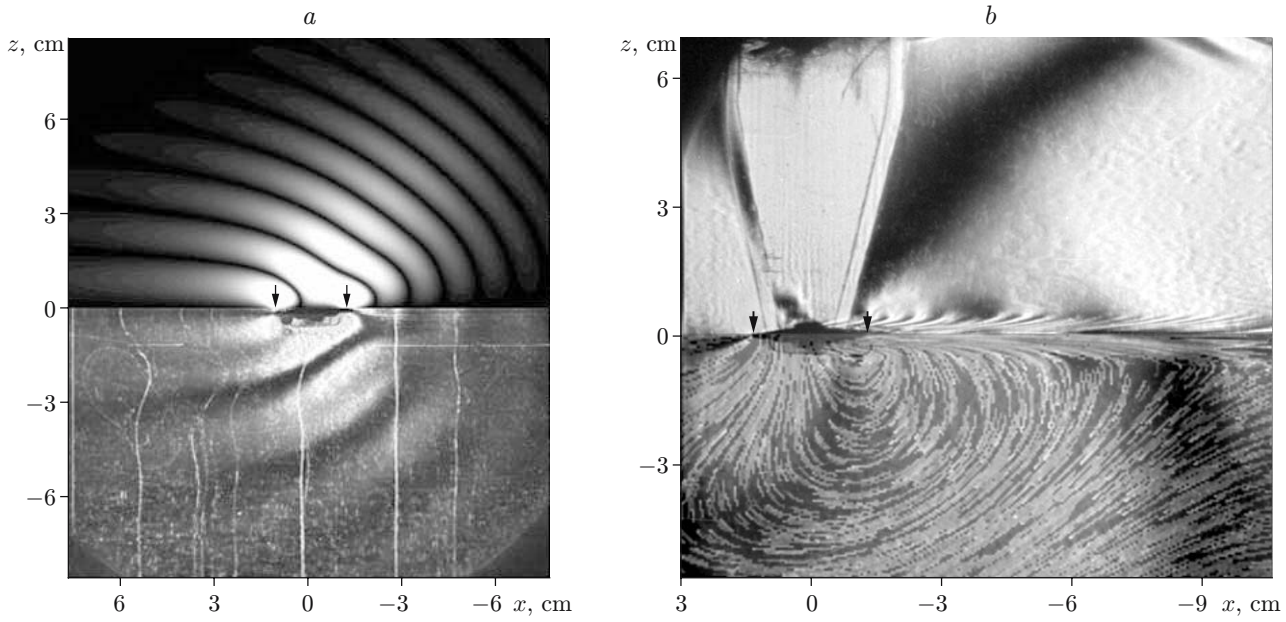

Fig. 3. Superimposed calculated and experimentally observed flow patterns near the short plate ($L_x = 2.5$ cm): (a) absolute value of the vertical velocity component (upper part of the figure) and the schlieren picture of the flow structure with density markers (lower part of the figure) ($U = 0.17$, $T_b = 14$ sec, Re = 42, Fr = 0.15, and $C = 1950$); (b) schlieren picture of the flow (upper part of the figure) with superimposed streamlines (lower part of the figure) ($U = 2.3$ cm/sec, $T_b = 7.55$ sec, Re = 575, Fr = 1.1, and $C = 570$); the arrows indicate the plate edges.

and troughs is a consequence of the Doppler effect and distortion of the original gradient, which is caused by the blockage effect. The experimental velocity of the fluid in the vicinity of the source plane is higher than the predicted value, which is manifested in greater displacements of the phase surfaces in the regions of contact with the wake.

If the plate length is substantially smaller than the wave length, the wave systems cannot be identified, and a global pattern of waves generated by a compact source is formed [6].

In the examined range of problem parameters, for both long and short plates (see Figs. 3 and 4), the calculated and experimentally observed phase surfaces almost coincide with each other and agree with the data obtained in [8]. This proves the adequacy of the linear model where the centers of wave generation are edge singularities. As the velocity is increased, nonlinear effects caused by the interaction of two systems of waves in the region of their intersection with each other and with singular components of the flow start to manifest themselves.

In an immediate vicinity of the plate, where the density gradients and velocity shear reach the maximum values, thin interfaces extended in the direction of motion are observed for all, even extremely small velocities of plate motion. For moderate velocities, a "rake" of shorter transverse streaky structures is formed in the vicinity of the short plate and in its near wake, in addition to extended streamwise interfaces (see Fig. 3b).

The fore parts of some streaks from a regular system of high-gradient structures are located at an angle of 3–10° to the horizon on the plate and almost horizontally behind the plate (see Fig. 3b); the angle between the streaks and the horizon increases with distance from the plane of motion. The streak thickness is 0.7–0.8 mm in the region of their formation, increases with distance from the plane of plate motion, and gradually becomes equal to half of the step of the structure. The plate image at the outer edge becomes smeared. The measurements performed show that the height of the region of streaky structures varies within 0.88 to 1.02 cm periodically increasing and decreasing with a scale defined by the length of attached internal waves $\lambda = UT_b$. Formation of such small-scale structures located symmetrically with respect to the plane of plate motion may be caused by the effect of edge singularities (see Fig. 1).

The frequency of repetition of individual finely structured elements, the number of streaky structures, and the total length of the region occupied by streaky structures depend on the size, velocity, buoyancy period, and angular position of the plate. For high values of velocity, the superimposed image of the flow near the plate (Fig. 5)

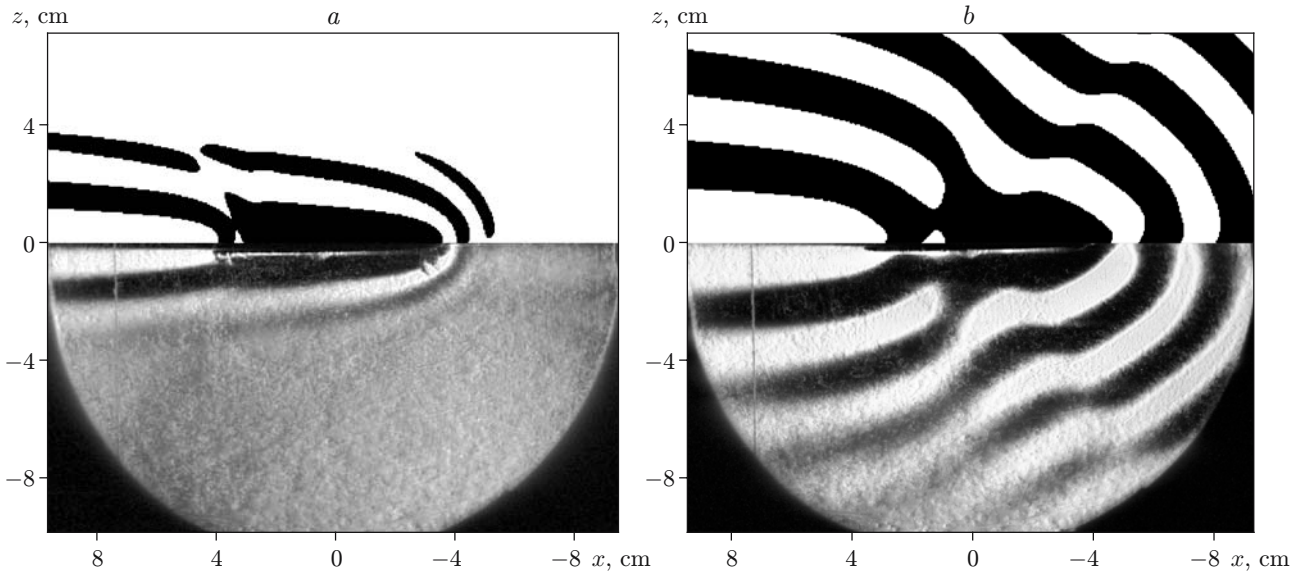

Fig. 4. Superimposed calculated fields of the signature of the vertical velocity component (upper part of the figure) and schlieren pictures of the experimentally observed flow patterns (lower part of the figure) near the long plate ($L_x = 7.5$ cm, $T_b = 7.6$ sec, and $C = 185$): (a) $U = 0.1$ cm/sec, Re = 75, and Fr = 0.016; (b) $U = 0.32$ cm/sec, Re = 240, and Fr = 0.05.

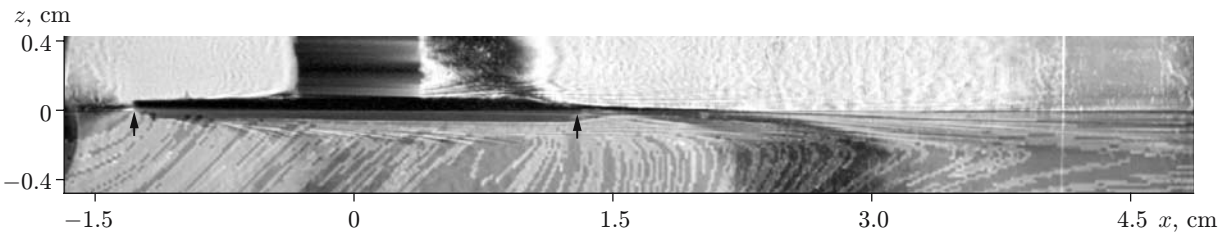

Fig. 5. Schlieren picture of the experimentally observed flow pattern (upper part of the figure) with superimposed streamlines (lower part of the figure) near the long plate ($L_x = 7.5$ cm, $T_b = 7.6$ sec, $U = 2.2$ cm/sec, Re = 1650, Fr = 0.35, and $C = 185$; the arrows indicate the plate edges).

whose length is greater than the viscous wave scale ($L_x \gg L_\nu$) also displays the same streaky structures as those observed near the short plate (cf. Figs. 5 and 3). In the present case, however, the streaks both on the plate and in the wake are predominantly aligned in the mean flow direction (Fig. 5) and coincide with the streamlines only in the wake behind the plate. The thickness of the streaks is less than 0.05 cm, i.e., lies at the boundary of the resolution of the schlieren instrument. In the fore part of the plate, alignment of the streamlines reflects the structure of the field of internal waves, whose geometry disagrees with the flow direction in the boundary layer. The angle of inclination of the streaks to the horizon near the long plate is 10°, and the height of the region occupied by streaky structures is 0.4 cm.

As the motion velocity is increased, regular streaky structures are grouped into clusters containing secondary short high-gradient interfaces, which form the outer boundary of vortices in the classical vortex street. Because of the suppressing effect of buoyancy forces, the vertical size of the vortex street ceases to grow rather rapidly. The flow is no longer homogeneous along the rays of light of the schlieren instrument, which pass parallel to the plate edges, i.e., the flow becomes unstable in the transverse direction and decomposes into a system of three-dimensional vortices [7].

The angular position of the plate substantially affects the pattern of internal waves and the wake structure. The lift force supplementing the drag force leads to displacement and relative shift of the phase surfaces of attached waves. In the tests whose results are illustrated in Fig. 6a, the trough of the first internal wave is located on

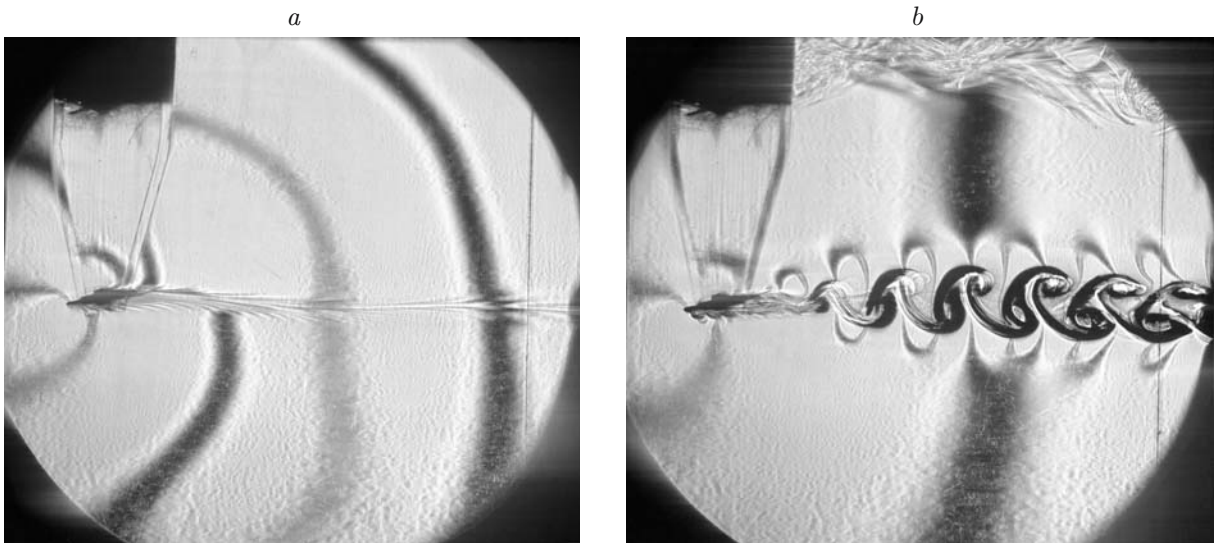

Fig. 6. Schlieren picture of the flow near an inclined plate (the diameter of the field of vision is 23 cm, $L_x = 2.5$ cm, $T_b = 7.55$ sec, $\alpha = 12.5^\circ$, and $C = 560$): (a) $U = 1.4$ cm/sec, Re = 350, and Fr = 0.67; (b) $U = 3.6$ cm/sec, Re = 900, and Fr = 1.73; the dark and light lines are the wave troughs and crests, respectively.

the leading edge of the plate in the upper half-space and contacts the lower surface at a distance of 0.9 cm from the leading edge. The first crest of the attached wave is adjacent to the trailing edge of the plate in the upper half-space. Near the wake behind the plate, the wave half-length is 6 cm in the upper half-space and 4.5 cm in the lower half-space, but here again the wake is split into individual extended interfaces.

The lift force distorts the wave field geometry: the crests and troughs are located symmetrically with respect to the plane of motion [or antisymmetrically behind the horizontal plate (see Figs. 3 and 4)]. The phase surfaces pass through the wake split into individual extended interfaces and through shorter inclined streaky structures. The dark and light lines (wave troughs and crests, respectively), beginning from the second one, come into contact in the wake region. The symmetrized phase structure of the wave field indices wavy oscillations of the density wake, which submerges as a whole into the troughs and emerges in the region of the crests of internal waves.

At low flow velocities, the pattern of the streaky structures above and below the inclined plate becomes essentially asymmetric. No streaks are observed on the windward side almost along the entire plate, except for the vicinity of its trailing edge. A system of short streaks extended in the direction of motion is adjacent to the wake–plate contact region. On the leeward side, the streaky structures are formed along the entire plate, beginning from the leading edge; some of the streaks are comparatively short, and others are fairly long. It should be noted that the streaks are thinner than those near the horizontally oriented plate (see Fig. 6a). In this regime, the height of the structured part of the flow is 0.8 cm.

The contrast of the image is indicative of high values of the density gradient in the region of streaky structures and, as a consequence, high values of the rate of baroclinic generation of vorticity [$\dot{\boldsymbol{\Omega}} = \nabla p \times \nabla (1/\rho)$] and kinematic vorticity $\boldsymbol{\Omega} = \operatorname{rot} \boldsymbol{v}$ ($\boldsymbol{v}$ is the fluid velocity). From the kinematic viewpoint, such structures can be interpreted as vortex layers and filaments. In systems with dissipation, the spatial scales of vorticity and density fields are of much lower order than the scales of variation of the velocity field [11]. The nonlinear interaction of compact structures with a high level of vorticity leads to formation of concentrated vortices and vortex systems. At the threshold of existence of these types of the flow, the process of vortex formation proceeds rather slowly, which makes it possible to trace its dynamics.

As the velocity is increased, the distances between individual transverse interfaces on the windward side of the plate become nonuniform. Three transverse vortex cores 0.4 cm in size are formed near the leading edge of the inclined plate; they transform to a rather thick wake (Fig. 6b) with protruding ends of the streaky structures. The wake becomes nonuniform in thickness and intensely oscillates in the vertical direction. The mid-points of the vortex cores of an asymmetric sequence of vortices (vortex street) are located at the points of wave turning. In

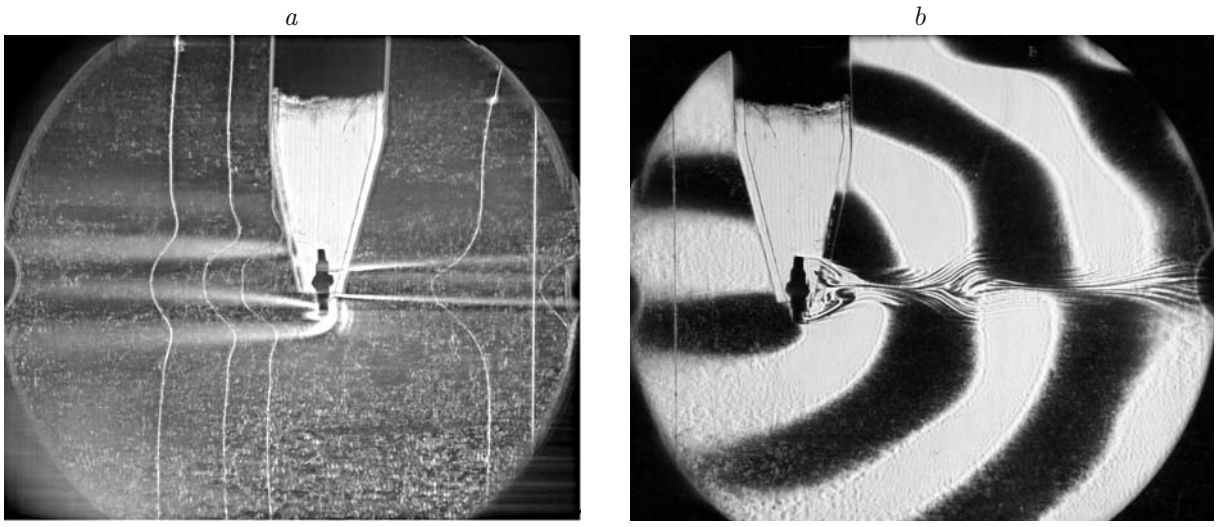

Fig. 7. Schlieren picture of the flow near the vertical plate (the diameter of the field of vision is 23 cm, $L_x = 2.5$ cm, $T_b = 17.4$ sec, and $C = 3000$): (a) $U = 0.033$ cm/sec, Re = 8.25, and Fr = 0.037; (b) $U = 0.29$ cm/sec, Re = 70, and Fr = 0.32.

this regime, the distance between the neighboring vortices (step of the street) is 2.4 cm; the flow geometry changes with distance from the plate. Thus, the cluster is symmetric in the center (see Fig. 6b), and the external edge of subsequent clusters enclosing the vortices are inclined in the direction of body motion. In the pair passing from the lower half-space to the upper half-space ($l_{x1} \approx 1$ cm along the horizontal line and $l_1 \approx 1.5$ cm between the centers of the vortices), the distances between the neighboring vortices are smaller than the distance in the pair passing from the upper half-space to the lower half-space (correspondingly, $l_{x2} \approx 1.4$ cm along the horizontal line and $l_1 \approx 1.9$ cm between the centers of the vortices). In this regime, the maximum vortex diameter is $d = 1.1$ cm. Stratification suppresses the increase in the vertical size of the wake already at a distance equal to half of the wave length from the trailing edge (in this experiment, $\lambda/2 = 10$ cm). The maximum vertical size of the wake is $h_{\max} = 2.4$ cm. In the right side of the image (see Fig. 6b), where the maximum "age" of the wake is $\tau = t/T_b = 0.7$, one can see that the vortices are flattened and levelled off.

Though the images of the vortex-street elements in Fig. 6b have a good contrast, magnification shows that the vortices consist of individual high-gradient elements. In regions of their superposition, the disturbances of the density gradient (and refractive index) become so intense that the light beams leave the dynamic range of the schlieren instrument. The image becomes vignetted with various structural elements. If the interfaces are split off, their thickness is smaller than 0.05 cm.

If the plate is aligned perpendicular to the flow, the wave pattern remains the same, but the character of the cocurrent flow becomes substantially different (Fig. 7). For low velocities of the vertical plate, upstream disturbances are clearly expressed, which include the blockage area ahead of the body, unsteady internal waves, and singular disturbances on the frontal side near the plate edges (the light spot on the frontal part of the lower edge). Above this spot, there is another inclined light interface inducing the outer boundary of the region of the blocked fluid (Fig. 7a).

The singular disturbance on the back part of the plate is distributed along the phase surface, which is a trough of the internal wave (light interface adjacent to the lower edge of the plate). Extended high-gradient interfaces, which are outer shells of the density wake, are adjacent to the back side of the plate at a distance of 0.8 cm from the outer edges. Their detachment from the plate edges means that the buoyancy effects are more clearly expressed in the deformed density field than the inertial effects. In this regime, the vertical size of the base vortex is smaller than the plate height, i.e., there is one more structural element of the flow between the wake and the plate edge (in this case, it is the edge singularity superimposed onto a short internal wave).

The contours of the deformed markers (thin vertical lines in Fig. 7a) visualize the vertical profiles of the horizontal velocity component. Ahead of the plate, the central part of the nearest marker is flat, which means

complete blockage of fluid motion in this region. The marker contours become smooth with distance from the plate, and the absolute value of their displacements decreases, which bears evidence of partial ventilation of this flow region. Ahead of the plate, the velocity shear layer thickness is $\Delta z_{up} = 1.1$ cm and the shear is $\partial u_x/\partial z = 0.055$ sec^{-1}; the local Richardson number $\mathrm{Ri} = N_0^2/(\partial u_x/\partial z)^2 = 230$ shows that the flow retains hydrodynamic stability.

The velocity wake whose size is characterized by the height of the density marker deformation region behind the plate is greater than the density wake. Its height in the vicinity of the density marker is $h_u = 4.5$ cm, while the height of the density wake is $h_d = 1.8$ cm ($h_u/h_d = 2.5$). The maximum velocity at the wake axis is approximately equal to the body velocity, the width of the velocity shear layer in the base wake is $\Delta z_{dw} = 1.1$ cm, the velocity shear is $\partial u_x/\partial z = 0.028$ sec^{-1}, and the Richardson number in the wake is $\mathrm{Ri} > 900$.

Accumulation of the fluid from the plane of motion ahead of the plate and its entrainment from the region behind the plate lead to reconstruction of the initially uniform density gradient. It becomes weaker in the region ahead of the plate and increases in the region behind the plate, thus, enhancing the effect of stratification on the base wake and vortex structures.

Owing to accumulation of vorticity and an increase in energy of vortex motion in the base part of the flow behind the plate, the outer shell of the density wake starts expanding, and its outer boundaries arrive on the plate edges (Fig. 7b). The wave disturbance becomes simpler and includes upstream unsteady waves and the interference pattern of attached waves caused by nonlocality of the generating disturbance. This disturbance includes not only the plate and the base vortex, but also the vortex elements inside the density wake.

The wake acquires a varicose shape and consists of vortex cores connected by a system of long interfaces extended in the mean flow direction. Thin interfaces in the wake are observed for a long time and disappear simultaneously with decay of larger-scale internal waves, which agrees with conclusions that the system of regular and singular components of stratified flows cannot be separated [10]. The positions of the extreme points of the density-wake boundary are rigorously synchronized with the phase pattern of attached internal waves. The minimum size of the vertical varicose density wake is observed in regions where the wave troughs in the upper half-space contact the wave crests in the lower half space. The maximum size, vice versa, is observed in regions where the wave crests in the upper half-space contact the wave troughs in the lower half-space. The efficiency of synchronization of the wave and vortex components is provided by the existence of a thin high-gradient shell of the wake.

Conclusions. Numerical visualization of the full solution of the linearized system of equations for a stratified fluid allows identification of regular (internal waves, upstream disturbance, and wakes) and singular (edge disturbances and boundary layers) components of the flow. In the experiment, the flow near the plate also consists of the regular (waves and vortices) and singular components (high-gradient interfaces — vortex surfaces and lines). High-gradient interfaces in the wake are observed for all velocities of plate motion.

At low velocities of plate motion, the pattern of internal waves is adequately described by linear models; the phase structures are in both qualitative and quantitative agreement with calculated results. Even in this regime, however, there exists one or several high-gradient interfaces, which are singular elements extended in the mean flow direction.

As the velocity is increased, transverse streaky structures (vortex surfaces or filaments) appear in the laminar wake behind the horizontal plate, in addition to streamwise interfaces. Formation of these streaky structures is caused by the action of edge singularities. With a further increase in velocity, the regular alignment of the streaky structures is violated, they are grouped into clusters, which are later transformed to vortex systems. Stratification suppresses the vertical motion and affects the vortex flow geometry. The number of elements, position, and extension of the region with streaky structures depend continuously on flow parameters in the range of their stable existence.

Nonlinear interaction of regular and singular elements of the flow violates the regular pattern of the streaky structures, favors formation of clusters, enhancement of the density gradient, formation of vortices and chains of vortices (vortex systems) both behind the horizontal plate and behind the inclined plate.

In the case of motion of the inclined plate, the effect of the lift force is manifested in changes in the phase structure of the field of internal waves and in the shape, size, orientation, and character of evolution of vortex systems. The wave field, which is antisymmetric near the inclined plate, may become symmetric in the upper and lower half-spaces.

If the plate is mounted perpendicularly to the motion direction, the features of the wave pattern remain unchanged, while the properties of the vortex pattern becomes substantially different. The wake split into individual interfaces acquires a varicose shape, the size and position of vortices in the wake being synchronized with the patter of attached internal waves.

This work was performed within the framework of Program No. OE-14 "Dynamics of Multiphase and Inhomogeneous Fluids" of the Department of Power Engineering, Mechanical Engineering, Mechanics, and Control Processes of the Russian Academy of Sciences and was supported by the Russian Foundation for Basic Research (Grant No. 05-05-64090) and by the Foundation for Supporting Domestic Science.

REFERENCES

1. L. D. Landau and E. M. Lifshits, *Course of Theoretical Physics*, Vol. 6: *Fluid Mechanics*, Pergamon Press, Oxford-Elmsford, New York (1987).
2. G. Schlichting, *Boundary Layer Theory*, McGraw-Hill, New York (1968).
3. J. Hoepffner, L. Brandt, and D. S. Henningson, "Transient growth on boundary layer streaks," *J. Fluid Mech.*, **537**, 91–100 (2005).
4. D. S. Sboev, G. R. Grek, and V. V. Kozlov, "Specific features of the internal structure of streaky structures," *Teplofiz. Aéromekh.*, **6**, No. 3, 381–392 (1999).
5. U. Ehresten and F. Gallaire, "On two dimensional models in temporal spatially evolving open flows: The flat boundary layer," *J. Fluid Mech.*, **536**, 209–218 (2005).
6. J. Lighthill, *Waves in Fluids*, Cambridge University Press, Cambridge (1978).
7. Yu. D. Chashechkin, V. V. Mitkin, and R. N. Bardakov, "Streaky structures in a stratified flow past a horizontal plate," *Dokl. Ross. Akad. Nauk*, **409**, No. 6, 774–778 (2006).
8. Yu. D. Chashechkin and V. V. Mitkin, "A visual study on flow pattern around the strip moving uniformly in a continuously stratified fluid," *J. Visual.*, **7**, No. 2, 127–134 (2004).
9. Yu. D. Chashechkin and Yu. V. Prikhod'ko, "Structure of flows formed by free oscillations of a cylinder on the horizon of neutral buoyancy in a continuously stratified fluid," *Dokl. Ross. Akad. Nauk*, **407**, No. 5, 622–625 (2006).
10. Yu. D. Chashechkin and A. V. Kistovich, "Classification of three-dimensional periodic flows in a fluid," *Dokl. Ross. Akad. Nauk*, **395**, No. 1, 55–58 (2004).
11. V. G. Baidulov, P. V. Matyushin, and Yu. D. Chashechkin, "Structure of a diffusion-induced flow around a sphere in a continuously stratified fluid," *Dokl. Ross. Akad. Nauk*, **401**, No. 5, 613–618 (2005).
12. Yu. D. Chashechkin and A. V. Kistovich, "Calculation of the structure of periodic flows in a continuously stratified fluid with allowance for diffusion effects," *Dokl. Ross. Akad. Nauk*, **393**, No. 6, 776–780 (2003).
13. A. Yu. Vasil'ev and Yu. D. Chashechkin, "Generation of beams of three-dimensional periodic internal waves by sources of various types," *J. Appl. Mech. Tech. Phys.*, **47**, No. 3, 314–323 (2006).
14. R. N. Bardakov and Yu. D. Chashechkin, "Calculation and visualization of two-dimensional attached internal waves in an exponentially stratified viscous fluid," *Izv. Ross. Akad. Nauk, Fiz. Atmos. Okeana*, **40**, No. 4, 531–544 (2004).
15. J. N. Newman, *Marine Hydrodynamics*, MIT Press, Cambridge (1977).
16. S. A. Smirnov, Yu. D. Chashechkin, and Yu. S. Il'inykh, "High-accuracy method for measuring the buoyancy period profile," *Izm. Tekh.*, No. 6, 15–18 (1998).